

International Conference on Space Optics—ICSO 2014

La Caleta, Tenerife, Canary Islands

7–10 October 2014

Edited by Zoran Sodnik, Bruno Cugny, and Nikos Karafolas



METIS-ESA solar orbiter mission internal straylight analysis

E. Verroi

V. Da Deppo

G. Naletto

S. Fineschi

et al.



icso proceedings



METIS- ESA SOLAR ORBITER MISSION INTERNAL STRAYLIGHT ANALYSIS

E. Verroi¹, V. Da Deppo², G. Naletto³, S. Fineschi⁴, E. Antonucci⁴

¹ *Centro Interdipartimentale Studi e Attività Spaziali (CISAS)–G. Colombo, University of Padova, Via Venezia 15, 35131 Padova Italy*

² *CNR-Institute for Photonics and Nanotechnologies UOS Padova LUXOR, Via Trasea 7, 35131 Padova Italy*

³ *Department of Information Engineering, University of Padova, Via Gradenigo 6/B, 35131 Padova Italy*

⁴ *INAF-Osservatorio Astronomico di Torino, Strada Osservatorio 20, 10025 Pino Torinese (TO), Italy.*

ABSTRACT

METIS is the Multi Element Telescope for Imaging and Spectroscopy for the ESA Solar Orbiter. Its target is the solar corona from a near-Sun orbit in two different spectral bands: the HI UV narrow band at 121.6 nm, and the VL visible light band. METIS adopts a novel inverted externally occulted configuration, where the disk light is shielded by an annular occulter, and an annular aspherical mirror M1 collects the signal coming from the corona. After M1 the coronal light passes through an internal occulter and is then reflected by a second annular mirror M2 toward a narrow filter for the 121.6 nm HI line selection. The visible light reflected by the filter is used to feed a visible light (580 – 640 nm) polarimetric channel. The photospheric light passing through the entrance aperture is back-rejected by a spherical rejection mirror.

Since the coronal light is enormously fainter than the photospheric one, a very tough suppression is needed for the internal stray light, in particular the requirement for the stray light suppression is more stringent in the VL than in the UV, because the emission of the corona with respect to the disk emission is different in the two cases, and the requirements are a suppression of at least 10^{-9} times for the VL and a suppression of at least 10^{-7} times for the UV channel.

This paper presents the stray light analysis for this new coronagraphic configuration.

The complexity of the optomechanical design of METIS, combined with the faintness of the coronal light with respect to the solar disk noise, make a standard ray tracing approach not feasible because it is not sufficient to stop at the first generation of scattered rays in order to check the requirements. Also scattered rays down to the fourth generation must be treated as sources of new scattering light, to analyze the required level of accuracy. If used in a standard ray tracing scattering analysis, this approach is absolutely beyond the computational capabilities today available; therefore we opted for a scattering ray generation with a Montecarlo method in which after a father ray hits a surface, only one ray is generated, randomly selected according to the distribution of the transmitted energy. These rays bring with them all the energy that is otherwise distributed between all the rays of second generation, making the model more realistic and avoiding loss of energy due to the rays sampling. The stray light has been studied in function of the mechanical roughness of the surfaces and the obtained results indicate an instrument stray light blocking performance well within the requirements in both channels.

I. SOLAR ORBITER

European Space Agency's Solar Orbiter (SO) is a mission dedicated to solar and heliospheric physics, in the framework of ESA's Cosmic Vision 2015-2025 Programme. SO will be devoted to the observation on how the Sun creates and controls the heliosphere; in particular one of the goals is to obtain new information about the solar wind, the heliospheric magnetic field, solar energetic particles, transient interplanetary disturbances and the Sun's magnetic field. The mission launch is scheduled in Jan 2017 and the spacecraft will have a high elliptic orbit, bringing the instruments up to 0.28 AU from the Sun, and it will make them able to acquire the first images from an out of the ecliptic orbit. Moreover, this specific orbit will allow a quasi-heliosynchronous observation period, making possible the investigation of low atmospheric structures, precluded for the near-Earth orbits.

The Multi Element Telescope for Imaging and Spectroscopy METIS is one of the ten instruments allocated in the SO [1]. A rendering of Payload accommodation onboard of Solar Orbiter is illustrated in Fig. 1.

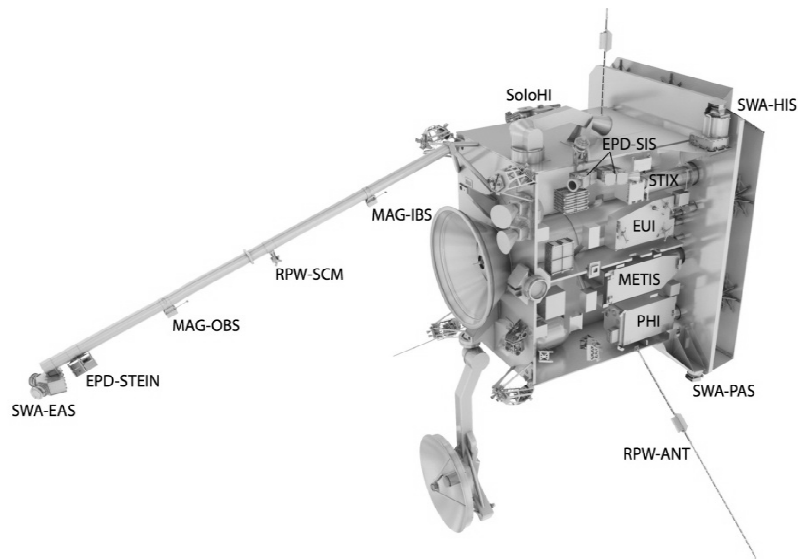


Fig. 1. Payload accommodation onboard Solar Orbiter. [2]. The other instruments indicated are: EPD: Energetic Particle Detector; MAG: Magnetometer; RPW: Radio and Plasma Waves; SWA: Solar Wind Plasma Analyser; EUI: Extreme Ultraviolet Imager; PHI: Polarimetric and Helioseismic Imager; SoloHI: Heliospheric Imager; SPICE: Spectral Imaging of the Coronal Environment; STIX: X-ray Spectrometer/Telescope

II. THE INSTRUMENT

METIS is solar coronagraph devoted to perform both visible and UV imaging. It incorporates the capability of observing the solar corona in two channels: a UV imaging channel in which the target (the solar corona) is imaged in the HI 121.6 nm line on the UV focal plane, and a visible light polarimetric channel, working in the 580 – 640 nm band.

METIS is conceived following a novel concept of *inverted* coronagraph, where the normal configuration of a coronagraph is replaced by a sort of dual design in which the external occulter is a hole and not a disk, and all the other elements are reversed by consequence (see [3] and [4] for further details). Fig. 2 depicts a schematic section of the instrument, in which the main elements are represented.

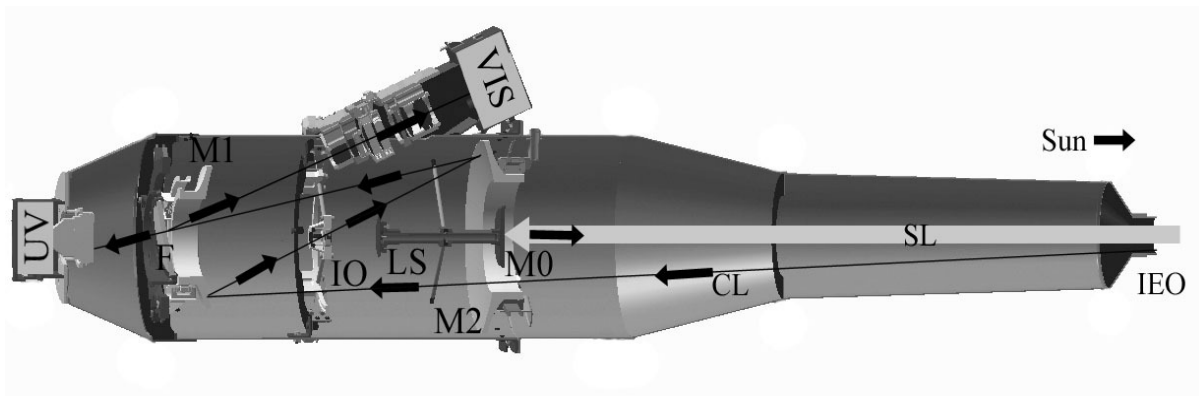


Fig. 2. Optomechanic structure of METIS. IEO is the Inverted external occulter, SL is the solar disk light incoming and rejected by the M0 rejection mirror, CL is the (coronal) light target. M1 and M2 constitute the on-axis gregorian telescope, UV and VIS are the detectors for the UV and visible channels, LS is a Lyot Stop and IO is the internal occulter. F is the Al+MgF₂ filter which splits the visible light and the HI line.

The radiation coming from the photosphere and the target enters through the inverted external occulter (IEO), a circular aperture in the spacecraft facing to the sun. The photospheric light (SL) is intercepted by a rejection mirror M0 and ejected from the IEO itself, while the coronal light (CL) is collected by an on-axis holed mirror M1. The first focal plane is located between M1 and a second mirror M2, where an occulter IO is placed in order to eliminate the IEO illuminated edge imaged there. A Lyot Stop LS, placed on the conjugate plane of M0 with respect to M1, is devoted to the suppression of the stray light scattered by the edge of M0 and reflected by

M1. Beyond M2 the light path is split in two different channels by means of an Al+MgF₂ filter, used for the selection of the HI line. The visible light reflected by the filter runs through the visible light polarimetric channel to the visible light detector (VIS in figure), while the UV radiation passes the filter towards the UV detector (UV in figure).

II. STRAY LIGHT ANALYSIS

A. Stray Light Requirements

Since the signal from the corona is many orders of magnitude fainter than the one coming from the sun disk, the suppression of stray light is essential to obtain a good resolution in the observations. The software estimation and verification of noise contributions arising from photospheric light prevents the risks of need for changes in the instrument opto-mechanical design and of intervention in the real instrument.

During the mission, SO will be orbiting at different distances from the Sun with the most critical configuration at the perihelion, in which SO will be at 0.28 AU from the Sun. In this condition the photosphere limb has the minimum angular distance from the instrument FOV (1.5 - 3 solar radii), so the photospheric spurious light is higher.

Our stray light analysis is performed considering the source only in the most critical position for the generation of diffuse light; this means that our source (the simulated Sun) is considered at the distance of 0.28 AU from the instrument.

The analysis is performed taking into account the different wavelength ranges at which the instrument works:

UV: Narrow band UV (HI 121.6 nm)

VL: Broadband polarized visible light VL (580-640 nm)

The average requirements on the in-band instrumental stray light (I_{stray}/I_{sun}) are:

$$\begin{aligned} I_{stray}(\text{VL}) &< 10^{-9} I_{sun} \quad (\text{VL: } 580 - 640 \text{ nm}) \\ I_{stray}(\text{UV/EUV}) &< 10^{-7} I_{sun} \quad (\text{UV: } 115 - 130 \text{ nm}) \end{aligned}$$

where I_{stray} represents the stray light irradiance level (photons/m² s) measured on the detector plane and I_{sun} represents the solar disk mean irradiance as seen by the same detector.

B. The Analysis Concept

Among the various options for the software analysis of stray light, we have chosen the most commonly used one, a ray tracing model taking into account single ray scattering from the various physical elements. The software used for the simulation is the Advanced Systems Analysis Program (ASAP ®) from Breault Research Organization, Inc. We have simulated via software the optical elements and the mechanical parts of interest. Obviously, the accuracy of the simulation also depends on how the physical properties of the diffusing objects hit by rays are reproduced.

As seen above, the intensity ratio between the disk light and the coronal light ranges between 10⁹ and 10⁷ (depending on the band) so also a tiny fraction of spurious light from the disk can heavily contaminate the vision of the coronal structures. Mainly due to this reason and to the complexity of the opto-mechanical design of METIS, a standard (brute force) ray tracing approach is a way not easily feasible. If one considers a beam of rays from the source into the instrument, for each "father" ray, millions of "son" rays have to be simulated after the scattering on a single surface, in order to achieve a good sampling of the stray light effects on the detectors. The requirements for the suppression of the stray light is quite stringent, so it is not sufficient to stop at the first generation of rays. That means for METIS even third generation scattered rays, or higher, can lead to relevant contributions to the photospheric noise, therefore also son rays should be treated as sources of scattering light and each of them should still give rise to millions of third generation rays. This approach is absolutely beyond the computational capabilities today available, if realistic numbers are considered - we used a source that has generated about 20 million rays.

Therefore we opted for a different approach (see also [5]). We have implemented a scattering ray generation with a Monte Carlo method: after a father ray hits a surface, only a few rays are generated, randomly selected according to the distribution of the transmitted energy. These rays bring with them all the energy that is otherwise distributed among all the second generation rays, making the model more realistic and avoiding loss of energy due to the rays sampling. The adopted stochastic approach allows to sample all the surfaces involved in the generation of possible stray light of higher order. Among the numerous rays coming from the simulated

Sun, when a surface is hit, the code considers the orientation of the surface imposed by the roughness and generates a son ray by using the normalized bidirectional scattering distribution function (BSDF) as a probability distribution (i.e. it is more likely that the ray is generated in the direction along which the BSDF is higher). The total energy reflected (usually divided by the number of son rays) is carried by the single ray generated.

Also when a scattered ray hits a new surface, the code randomly generates a new ray, selected according to the distribution of the transmitted energy. The process can be stopped either after a certain value of scatter order or when the single ray has fallen below an energy threshold.

For the visible channel we considered $\lambda = 600$ nm as reference wavelength, and a square source in front of the entrance aperture composed by a grid of 5000×5000 rays, so that a beam composed by approximately 19 millions of rays enters the instrument. The rays are emitted within an angular aperture of 0.95° , that is the angular radius of the sun seen by METIS at the perihelion.

The UV channel considers a grid of 4600×4600 for a $\lambda = 121.6$ nm and the same angular aperture of the beam.

C. Modeling the optomechanics

The accuracy of the analysis depends largely on how the mathematical representation of the objects involved in the scattering processes corresponds to the real behavior of the physical objects. In particular on how the scattering properties are simulated and how the "real-world" surfaces are modeled. Hereinafter we briefly describe the modeling of the physics in our simulation.

In order to investigate the superficial roughness of the used materials we simulated three different micro-roughness types for all the scattering surfaces for both UV and VIS channels.

The parameter used for the description of a physical surface taken into consideration is the average roughness R_a . If we consider sampling region on the material surface having a length L and a function which describes the surface one-dimensional profile $z(x)$, R_a will be described by

$$R_a = \frac{1}{L} \int_0^L |z(x)| dx$$

In particular we simulated a surface roughness with the following parameters:

R1: $R_a = 0.1 \mu\text{m}$ corresponding to a perfectly smooth surface obtained with lapping process

R2: $R_a = 1.0 \mu\text{m}$ corresponding to a extra-fine grinding for machine tools

R3: $R_a = 3.0 \mu\text{m}$ corresponding to a smooth grinding for machine tools

The roughness simulation assigns to the surface random gaussian distributed heights around the chosen parameter. At the base of the roughness model there are two assumptions: the isotropy of the surface and the stationarity of the autocorrelation length of the surface profile (the profile function does not change with the direction considered on the surface and neither with the position on the surface, essentially it depends only on the relative distance between two points on the surface).

The roughness simulation assigns a certain variation of the surface orientation in micro zones of the surface itself. When a single rays hit a point on this surface we simulate the response of the body to the incoming light, that depends on the physical properties of the material under analysis. In our study, these properties have been described by an isotropic scattering function which depends on the angle of incidence of the radiation (θ_i) and on the transmission angles (θ_r, φ) in terms of the BSDF ($\theta_i, \theta_r, \varphi$) (here we do not consider the second incidence angle φ_i since we are in isotropic approximation).

The BSDF (θ) considered for the black coating of the mechanical elements simulated in our analysis is shown in Fig. 3 The panel returns the value of BSDF for some values of the incidence angle θ_i .

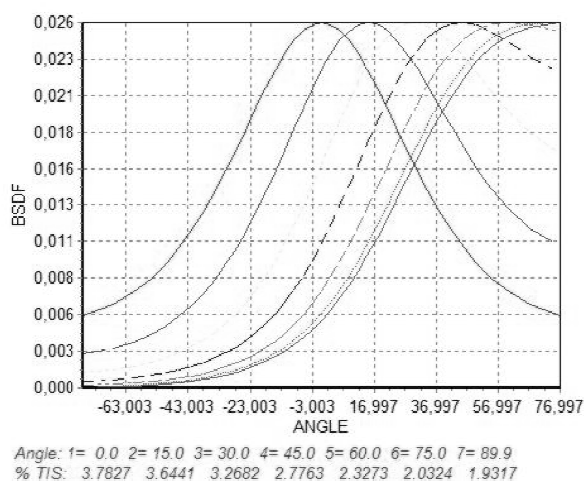


Fig.3. BSDF for the black coating considered for the mechanical elements for different incidence angles (in degrees).

The optical elements have been simulated as polished mirrors having a surface roughness of $\lambda/30$, while the volume scattering due to the dioptric elements (glass imperfection etc) has not been considered in this analysis.

D. Analysis Results

At the end of the process, a residual part of the solar disk light survives the rejection by M0, the internal occultation of the IEO edge, the Lyot Stop suppression, the Field Stops cut off and the absorption by the instrument structure, and hits the detector together with the target radiation. In order to compute the level of noise given by this residual stray light, we considered its amount compared with the original flux from the solar disk in a certain band.

If the simulated beam from the disk is composed by N rays, the total beam energy is \mathcal{E} and each single first generation ray carries an energy equal to $1/N$ of the total, that is \mathcal{E}/N . To reduce the calculation time, a threshold value of 10^{-15} in the energy carried by the single ray has been set together with a limit of a 6th generation of scatter; beyond these thresholds the single ray is suppressed and it is no longer taken into account in the simulation.

The number of rays surviving the multiple scatters multiplied by their intensities is integrated over the detectors surfaces and then compared with the number of rays of intensity 1 that would reach the detector if it were directly illuminated by the disk radiation (the stray light intensity is normalized to the disk emission intensity).

All this process, as already mentioned above, was repeated for three different values of the surface roughness. In the visible channel the total flux integrated on the detector surface indicate a value slightly dependent on the roughness. In particular for the three roughness amplitude indicated, the simulation returns

Average roughness considered	Total noise intensity on the detector normalized to initial flux ()
R1: 0.1 μm	8.30E-12
R2: 1.0 μm	2.38E-11
R3: 3.0 μm	3.07E-11

Fig. 4 shows the dependence of the detected stray light on the value of the surface roughness parameter, while Fig. 5 indicates the position of survived scattered rays impinging the VIS detector.

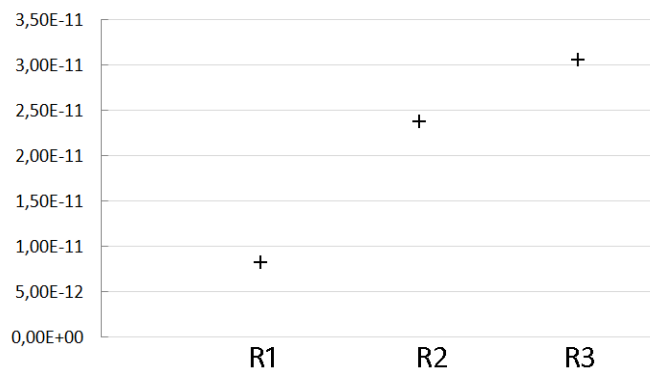


Fig. 4. Total flux of stray light on the detector in fraction of the photospheric flux entering the instrument for the VIS channel. The graphic shows the results in function of the three roughness parameter considered (0.1; 1; 3 μm).

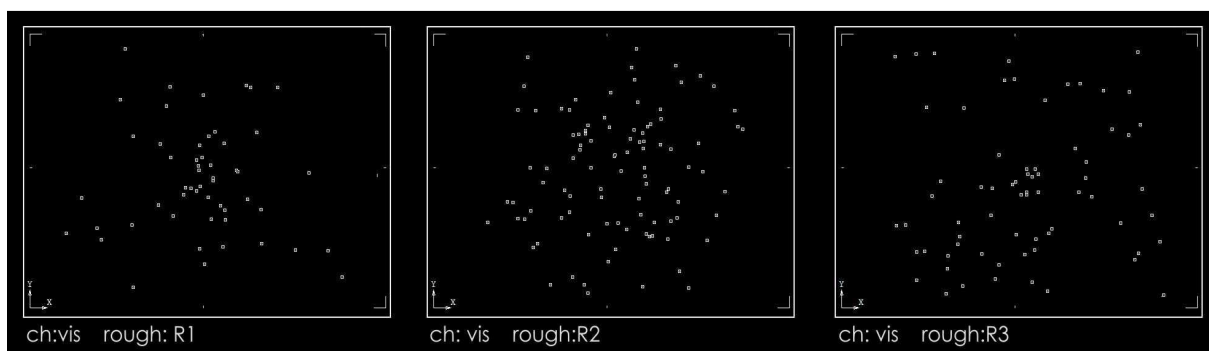


Fig. 5. Straylight rays on the detector for the VIS path for the three roughness parameter considered.

The same analysis for the UV 121.6nm channel returns the results shown below. The dependence found for the intensity of stray light on the roughness of the mechanical and optical surfaces is shown in Fig. 6 and in Fig. 7. The positions of the scattered rays that reach the UV detector are indicated.

Average roughness considered R_a	Total noise intensity on the detector (normalized to initial flux ϵ)
R1: 0.1 μm	8,06E-10
R2: 1.0 μm	8,82E-10
R3: 3.0 μm	9,25E-10

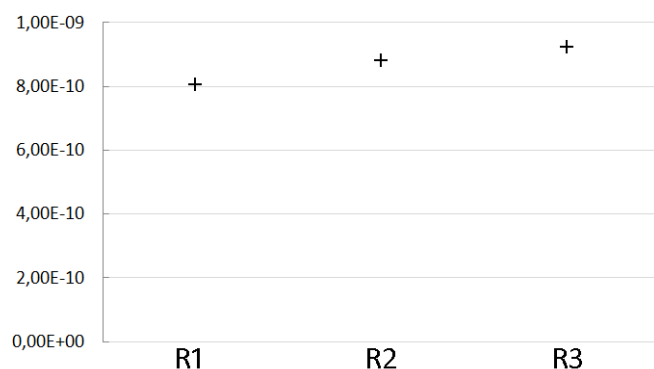


Fig. 6. Total flux of stray light on the detector in fraction of the photospheric flux entering the instrument for the UV channel in function of the three roughness parameters considered (0.1; 1; 3 μm)

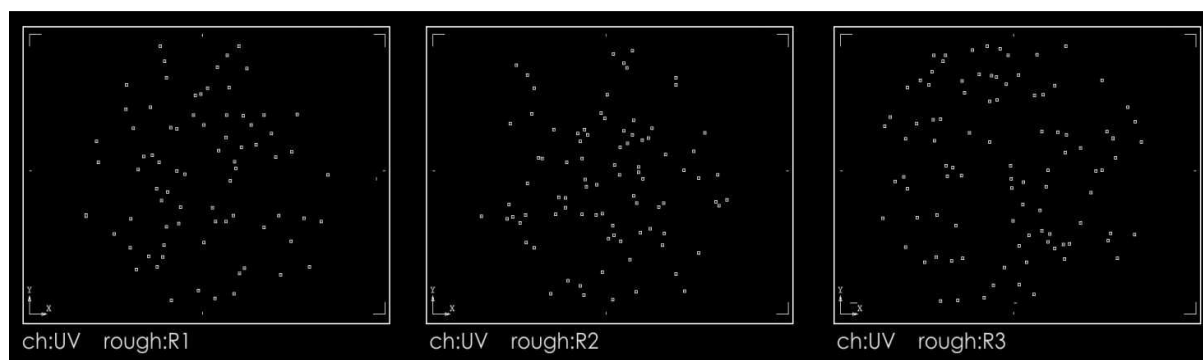


Fig. 7. Image of ‘straylight’ rays incident on the detector for the UV path.

The difference between the straylight for the UV and VIS detectors is larger than one order of magnitude and it is mainly attributed to the different position of the detectors in the instrument architecture and the following greater shielding of the VIS detector. Also with the dependence on the roughness, the simulated instrument performances are well within the requirements in both channels.

However further analysis has to be performed in the future in order to evaluate the contribution of the optics degradation in space environment and the possibility of off-band stray light.

REFERENCES

- [1] ESA/SRE, “Solar Orbiter, Assessment study report”, December 2009.
- [2] Credit: ESA: <http://sci.esa.int/solar-orbiter/51217-instruments/>
- [3] S. Fineschi, Novel Optical Designs for Space Coronagraphs: Inverted Occulters and Lyot-stops, proc. of ICSO Conference, Oct. 2010.
- [4] S. Fineschi, Inverted-COR: Inverted-Occultation Coronagraph for Solar Orbiter, Technical Note n. 119, Osservatorio Astronomico di Torino, 2009.
- [5] E. Verroì ; V. Da Deppo ; G. Naletto ; S. Fineschi ; E. Antonucci, Preliminary internal straylight analysis of the METIS instrument for the Solar Orbiter ESA mission *Proc. SPIE* 8442, Space Telescopes and Instrumentation 2012: Optical, Infrared, and Millimeter Wave, 84424N (August 22, 2012); doi:10.1117/12.926485